UNIVERSIDADE FEDERAL DO ESPÍRITO SANTO

CENTRO DE CIÊNCIAS AGRÁRIAS E ENGENHARIAS

PROGRAMA DE PÓS-GRADUAÇÃO EM GENÉTICA E MELHORAMENTO

ARIANE TONETTO VIEIRA

Copia LTR-retrotransposon superfamily occurrence and distribution and its role in the nuclear and chromosomal DNA content variations in two *Passiflora* species

ALEGRE

2018

ARIANE TONETTO VIEIRA

Copia LTR-retrotransposon superfamily occurrence and distribution and its role in the nuclear and chromosomal DNA content variations in two *Passiflora* species

Dissertação apresentada à Universidade Federal do Espírito Santo como requisito parcial para obtenção do Título de Mestre pelo Programa de Pós-Graduação em Genética e Melhoramento.

Orientador: Dr. Wellington Ronildo Clarindo

ALEGRE

2018

Dados Internacionais de Catalogação-na-publicação (CIP)
(Biblioteca Setorial Sul, Universidade Federal do Espírito Santo, ES, Brasil)

Vieira, Ariane Tonetto, 1994-

V657c Copia LTR-retrotransposon superfamily occurrence and distribution and its role in the nuclear and chromosomal DNA content variations in two Passiflora species / Ariane Tonetto Vieira. – 2018.

42 f. : il.

Orientador: Wellington Ronildo Clarindo.

Coorientador: Maria Andréia Corrêa Mendonça ; Fernanda Aparecida Ferrari .

Dissertação (Mestrado em Genética e Melhoramento) – Universidade Federal do Espírito Santo, Centro de Ciências Agrárias e Engenharias.

1. Maracujá. 2. Cariótipos. 3. Cromossomos. 4. Genoma. I. Mendonça, Wellington Ronildo Clarindo. II. Mendonça, Maria Andréia Corrêa. III. Ferrari, Fernanda Aparecida. IV. Universidade Federal do Espírito Santo. Centro de Ciências Agrárias e Engenharias. V. Título.

CDU:631.523

Bibliotecário: Felicio Gomes Corteletti – CRB-6 ES-000646/O

ARIANE TONETTO VIEIRA

***Copia* LTR-retrotransposon superfamily occurrence and distribution and its role in the nuclear and chromosomal DNA content variations in two *Passiflora* species**

Dissertação apresentada à Universidade Federal do Espírito Santo como requisito parcial para obtenção do Título de Mestre pelo Programa de Pós-Graduação em Genética e Melhoramento.

27 de julho de 2018.

Comissão Examinadora:

Wellington Ronildo Clarindo

Prof. Dr. Universidade Federal de Viçosa

(orientador)

Milene Miranda Praça-Fontes

Profa. Dra. Universidade Federal do Espírito Santo

(membro interno)

Maria Andréia Corrêa Mendonça

Profa. Dra. Instituto Federal Goiano – Rio Verde

(membro externo)

Guilherme Mendes de Almeida Carvalho

Prof. Dr. Instituto Federal do Norte de Minas Gerais (membro externo)

A Deus,

Aos meus pais Sérgio e Graça (in memoriam), meu irmão Matheus, e meus avós Paulo e Luzia por todo apoio durante minha vida e minha formação.

Dedico

AGRADECIMENTOS

A Deus por me conceder sabedoria e força durante a minha caminhada.

À Universidade Federal do Espírito Santo pelo apoio logístico no desenvolvimento desse projeto e ao Programa de Pós-Graduação em Genética e Melhoramento;

À FAPES (Fundação de Amparo à Pesquisa do Espírito Santo) pela concessão da bolsa e pelo financiamento da pesquisa a qual esse trabalho está vinculado;

Ao meu orientador, professor Dr. Wellington Ronildo Clarindo, pelos ensinamentos concedidos, os quais auxiliaram no meu desenvolvimento científico.

Às minhas coorientadoras Dra. Fernanda Aparecida Ferrari Soares, pelo ensinamento acerca da citogenética molecular, e professora Dra. Maria Andréia Corrêa Mendonça, pela disponibilidade em sempre me ajudar desde o pré-projeto.

À professora Dra. Milene Miranda Praça Fontes, pelo apoio e ensinamentos durante minha graduação e mestrado.

Aos membros da Banca Examinadora, professores Milene Miranda Praça Fontes, Maria Andréia Corrêa Mendonça e Guilherme Mendes de Almeida Carvalho, por terem aceitado o convite para participar, contribuindo com sugestões para a melhoria do trabalho.

Ao professor Carlos Roberto de Carvalho (UFV), pela contribuição nas análises de citometria de fluxo.

A todos os professores, pelos ensinamentos que contribuíram para o meu crescimento acadêmico, profissional e pessoal.

Aos técnicos Hamon e Soninha, pela disponibilidade em sempre me ajudar.

Aos colegas dos Laboratórios de Citogenética e Cultura de Tecidos e de Genética e Melhoramento Vegetal, por participarem no desenvolvimento desta pesquisa, tornando-a mais alegre e

descontraída. Em especial à Cristiana, pelo apoio nas análises moleculares, ao Lucas, pela ajuda com os primers.

À minha família, pelo amor e apoio incondicional, meu pai Sérgio, meu irmão Matheus e meus avós Paulo e Luzia, por acreditarem que o meu sonho pudesse se tornar real. Dedico minha conquista a vocês.

Ao meu melhor amigo e namorado, Adan, pelo amor, alegria, companheirismo, apoio, compreensão e paciência em todos os momentos.

Aos meus amigos Natália, Stéfanie, Victor e Darley, pelo apoio, paciência, conselhos, troca de conhecimentos e todos os nossos momentos de risadas sem fim.

BIOGRAFIA

Ariane Tonetto Vieira, filha de Milton Sérgio Vieira e Maria das Graças Tonetto Vieira (in memoriam), nasceu em Vitória, Espírito Santo, no dia 25 de março de 1994. Em 2012, ingressou na Universidade Federal do Espírito Santo, em Alegre, ES, graduando-se Bacharela em Ciências Biológicas em Agosto de 2016. Durante o período de graduação foi bolsista de iniciação científica PIBIC/CNPq, tendo desenvolvido atividades de pesquisa nas áreas de citogenética vegetal, de cultura de tecidos e de citometria de fluxo. Em agosto de 2016 iniciou o Mestrado no Programa de Pós-graduação em Genética e Melhoramento da Universidade Federal do Espírito Santo, atuando na área de Biologia Evolutiva e Citogenética, sob orientação do Prof. Dr. Wellington Ronildo Clarindo, submetendo-se à defesa de dissertação em julho de 2018.

LISTA DE ABREVIATURAS

APM – Amiprophos-methyl

BAC – Bacterial artificial chromosome

BES – BAC- end sequence

DAPI – 4', 6-diamidino-2-phenylindole

FCM – Flow cytometry

FISH – Fluorescent in situ hybridization

ICM – Image cytometry

IOD – Integrated optical density

LTR – Long terminal repeat

LTR-RT – Long terminal repeat retrotransposon

PBS – Phosphate buffer saline

PCR – Polymerase chain reaction

rDNA – ribosomal RNA

SD – Standard deviation

SSC – Sodium citrate

YR – Tyrosine recombinase

LISTA DE FIGURAS

LISTA DE TABELA

SUMÁRIO

Article: *Copia* LTR-retrotransposon superfamily occurrence and distribution and its role in the nuclear and chromosomal DNA content variations in two *Passiflora* species.

Authors: Ariane Tonetto Vieira[1], Fernanda Aparecida Ferrari Soares[2], Cristiana Torres Leite[1], Maria Andréia Corrêa Mendonça[3], Wellington Ronildo Clarindo[2]✉

[1]Laboratório de Citogenética e Cultura de Tecidos, Departamento de Biologia, Centro de Ciências Agrárias e Engenharias, Universidade Federal do Espírito Santo. ZIP: 29.500-000 Alegre – ES, Brazil.

[2]Laboratório de Citogenética e Citometria, Departamento de Biologia Geral, Centro de Ciências Biológicas e da Saúde, Universidade Federal de Viçosa. ZIP: 36.570-900 Viçosa – MG, Brazil.

[3]Laboratório de Biotecnologia, Instituto Federal Goiano – Campus Rio Verde. ZIP: 75.901-970 Rio Verde –GO, Brazil.

✉Corresponding author: e-mail: well.clarindo@ufv.br

Tel.: +55 31 3899-2568, FAX: +55 31 3899-1296

Resumo

Semelhante a outras espécies de *Passiflora*, a variação do conteúdo de DNA nuclear ocorre entre *Passiflora edulis* e *Passiflora quadrangularis* que possuem o mesmo número 2n de cromossomos. Para algumas espécies, esta variação se acumula distintamente entre os cromossomos, sendo os elementos retrotransponíveis uma das causas. Entre os retroelementos, os retrotransposons LTR constituem uma fração significativa dos genomas, desempenhando um papel importante na evolução do cariótipo. Este estudo visa investigar a ocorrência e distribuição dos retrotransposons LTR da superfamília *Copia* em cromossomos de *P. edulis* e *P. quadrangularis*, e entender o papel dessas sequências nas variações do conteúdo de DNA nuclear e cromossômico. Corroborando com a origem monofilética das espécies, os cariótipos apresentaram o mesmo número de cromossomos, predominância de cromossomos metacêntricos e submetacêntricos, e dois cromossomos com o rDNA 18S na porção terminal dos braços curtos e longos. A evolução do cariótipo foi evidenciada pelo papel do retrotransposon LTR nas diferenças de conteúdo de DNA nuclear e cromossômico entre as espécies, sendo este retroelemento distribuído de maneira diferente e aleatória entre todos os cromossomos. A identificação inequívoca de cada cromossomo por meio da morfometria, rDNA 18S, conteúdo de DNA e retrotransposons LTR também mostrou que, individualmente para o cariótipo de *P. edulis* e *P. quadrangularis*, não há relação entre o comprimento total e o conteúdo de DNA em alguns cromossomos. Esse fenômeno ocorreu nos cromossomos 2 e 6 de *P. edulis* em relação aos cromossomos 1 e 5, respectivamente, e no cromossomo 8 de *P. quadrangularis* para o cromossomo 7. Buscando o refinamento da metodologia citogenética, este estudo evidenciou cada cromossomo de *P. edulis* e *P. quadrangularis*, mostrando algumas alterações cariotípicas e os resultados promovidos pelos retrotransposons LTR.

Palavras-chave: maracujá, evolução do cariótipo, cromossomo, tamanho do genoma, retroelementos.

Abstract

Similar to other *Passiflora* species, nuclear DNA content variation occurs between *Passiflora edulis* and *Passiflora quadrangularis*, which show the same 2n chromosome number. For some species, this variation accumulates distinctly in the chromosomes, with retrotransposable elements being considered one of the causes for this observed variation. LTR-retrotransposons (LTR-RT) constitute a substantial portion of the genomes, playing an important role in karyotype evolution. This study aims to investigate the occurrence and distribution of the *Copia* LTR-RT superfamily in *P. edulis* and *P. quadrangularis* chromosomes, and to understand the role of these sequences in nuclear and chromosomal DNA content variations. The karyotypes showed the same chromosome number, predominance of metacentric and submetacentric chromosomes, as well as 18S rDNA in the terminal portion of the short and long arms of two chromosomes, corroborating the monophyletic origin of the species. The role of LTR-RT in karyotype evolution was evidenced by differences in nuclear and chromosomal DNA content between the species as well as differently and randomly distributed retroelements between all chromosomes. Unambiguous identification of each chromosome by morphometry, 18S rDNA, DNA content and LTR-RT allowed us to show that there is no relation between the total length and DNA content for some chromosomes. This phenomenon occurred in *P. edulis* chromosomes 2 and 6 in relation to chromosomes 1 and 5, respectively, and in *P. quadrangularis* chromosome 8 compared to 7. Using refined cytogenetic approaches, we analyzed each chromosome of *P. edulis* and *P. quadrangularis* individually, finding that karyotype changes were promoted by LTR retrotransposons.

Keywords: Passionfruit; Karyotype evolution; Chromosome; Nuclear genome size; Retroelements.

Introduction

Passiflora L. is the most representative subgenus of the *Passiflora* L. genus, comprising species with x = 9 and x = 10 chromosomes. This subgenus is a good taxon to study the causes of the nuclear genome size variation, since species with the same basic chromosome number (x = 9) have marked differences in nuclear DNA content, specifically 1C = 1.25 pg for *Passiflora edulis* Sims (Yotoko et al. 2011) and 1C = 2.68 pg for *Passiflora quadrangularis* L. (Souza et al. 2008). This variation can be related to differences between the karyotypes, which may be accumulated in distinct chromosomes, thus promoting chromosomal DNA content variation. So, it is important to characterize each chromosome pair by classical cytogenetics, and use additional tools to provide quantitative data on the DNA content of each chromosome. Hence, this study focused on two questions: is the nuclear genome size variation evenly distributed among all chromosomes of *P. edulis* and *P. quadrangularis*? Conversely, are there chromosomes containing more DNA than others?

Nuclear DNA content variation in plants can occur due to distinct events, such as the accumulation and/or elimination of repetitive DNA sequences (Bennetzen and Wang 2014). A significant contribution to the evolution of the genome size in plants is related to class I transposable elements, called retrotransposons (Bennetzen and Wang 2014). Retrotransposons can be divided into four groups: Long Terminal Repeat retrotransposons (LTR-RT), Non-LTR retrotransposons, Tyrosine Recombinase retrotransposons, and Penelope retrotransposons (Eickbush and Jamburuthugoda 2008). The majority of the LTR-RT belongs to either *Copia* or *Gypsy* superfamilies (Heslop-Harrison and Schwarzacher 2011). These elements are abundant in plants, for example comprising 75% of the total genome of *Zea mays* L. (Schnable et al. 2009), 62% in *Solanum lycopersicum* L. (Paz et al. 2017), or 20% in *Arabdopsis thaliana* L. (Underwood et al. 2017). In *P. edulis*, the LTR-RT correspond to 17.6% (~1.83 Mb) of sequenced genome data, equivalent to about 1% (10.4 Mb) of the total genome size (Munhoz et al. 2018). LTR-RT occurrence leads us to question the role of these elements in the nuclear and in chromosomal DNA content variations among monophyletic taxa. Therefore, a third question arises: might the possible variations in nuclear and chromosomal DNA contents in *P. edulis* and *P. quadrangularis* be due to LTR-RT occurrence?

LTR-RT play a structural role in the heterochromatin between telomere and centromere portions (Bennetzen 2000; Gao et al. 2008; Bierhoff et al. 2013; Li et al. 2017), as well as in the centromere

(Castro Nunes et al. 2018), telomeres (Zou et al. 2009), knobs (Díez et al. 2013) and chromomeres (Chang et al. 2008). As functional component of the centromere heterochromatin, LTR-RT contribute to the kinetochore structure, which is a fundamental chromosome portion for microtubule association and chromosome and chromatid segregation during anaphases (Freeling et al. 2015). In addition, these retroelements can interfere in gene expression, when their insertion occurs close to genes, promoting epigenetic changes (Bierhoff et al. 2013; Vicent and Casacuberta 2017). Uncontrolled amplification of LTR-RT can expand heterochromatin domains in plants, as reported for *A. thaliana* in which pericentromeric heterochromatin has been expanded 6 to 10 times in the last 5 million years (Hall et al. 2006). Given the amount of LTR-RT observed in different plant taxa and the structural and functional roles of these elements, the knowledge of the physical location of these sequences in each chromosome could help us to understand the importance of these sequences in karyotype evolution. Besides, this knowledge is important to interpret the differences in nuclear DNA contents between species, as observed in *Passiflora*.

The *Copia* LTR-RT superfamily is randomly located in genomes, but it can frequently be found in heterochromatic regions of the plant chromosomes. These elements can exhibit a block distribution in subterminal and telomeric regions, as seen in *Erianthus arundinaceu*s Hainan chromosomes (Huang et al. 2017), or, conversely, a dispersed distribution in the centromeric and pericentromeric regions as in *Coffea canephora* Pierre ex Froehner, *Coffea eugenioides* S. Moore and *Coffea arabica* L. chromosomes (Castro Nunes et al. 2018). In addition, retrotransposons can be distributed evenly throughout, as in euchromatin in *Z. mays* (Mroczek and Dawe 2003) and in *Solanum lycopersicum* (Xu and Du 2014) chromosomes. Although these studies mark the chromosomal regions in which the LTR-RT occur, most of them do not assemble the karyogram in order to indicate which chromosomes hold these transposable elements. So, to address the questions of this study and to map the LTR-RT, morphometric characterization and DNA content of each chromosome were provided. We also used an 18S rDNA marker was used for unambiguous identification of individual chromosomes.

In this context, image cytometry (ICM) can be used as an additional tool for karyotype characterization (e.g. *Z. mays*, Rosado et al. 2009; Silva et al. 2018). Associating cytogenetic and ICM approaches, *Z. mays* 'Black Mexican Sweet Corn' individuals were intraspecifically discriminated based on DNA content of each chromosome of the A and B complements, leading to distinguished variations in

DNA content that amounted to 1C = 0.045 pg (Rosado et al. 2009). In another ICM study, Silva et al. (2018) updated the *Z. mays* 'AL Bandeirante' karyotype from the descriptive to the quantitative level by estimating the DNA content of all chromosomes as well as their long and short arms, and the satellite of the chromosome 6. They found that the DNA content of chromosome 9 (1C = 0.280 pg) was higher than of chromosome 8 (1C = 0.266 pg), a fact associated to the occurrence of the knob in the long arm of the chromosome 9. In this species, retrotransposons are abundant in the heterochromatin knobs, with knobs being related to genome size increase (Díez et al. 2013).

Using cytogenetic tools, our study provides a karyotype refinement of two *Passiflora* species, by means of: (a) morphometric characterization of each chromosome, (b) measurement of the nuclear and chromosomal DNA contents, (c) mapping of 18S rDNA sites, and (d) identifying of the LTR-RT sequences of the *Copia* superfamily on the karyotypes of *P. edulis* and *P. quadrangularis*. The results showed the occurrence of the *Copia* LTR-RT superfamily in *P. edulis* and *P. quadrangularis* chromosomes, evidencing one relevant cause of the nuclear and chromosomal DNA content variations. Together, these findings provide important insights into the karyotype evolution of species with the same 2n chromosome number.

Materials and methods

Plant material

Fruits of *Passiflora edulis* (Voucher – 34970) and *P. quadrangularis* (Voucher – 34962), *Passiflora* subgenus, were collected in the experimental area of the Universidade Federal do Espírito Santo, Campus Alegre, Brazil (20 45' 49" S, 41 31' 58" W). *P. edulis* and *P. quadrangularis* were chosen because they exhibit (a) the same basic chromosome number, x = 9, as revealed by our previous classical cytogenetic studies, and (b) contrasting nuclear DNA contents (Souza et al. 2008; Yotoko et al. 2011). Flow cytometry was conducted in order to confirm the difference in nuclear DNA content between the species. For this, *Solanum lycopersicum* L. 'Stupické' seeds were used as internal standard (2C = 2.00 pg, Praça-Fontes et al. 2011).

In vitro plantlets

P. quadrangularis and *P. edulis* seeds were manually scarified to remove the pericarp using a scalpel. The seeds were disinfested in a laminar flow chamber by immersion in 70% ethanol for 20 s, then for 20 min in 1.5% commercial sodium hypochlorite containing Tween 20 (Sigma®), one drop for every 100 ml. The seeds were washed four times in distilled/deionized/sterilized water, dried in sterilized filter-paper, and inoculated in germination medium composed of 2.15 g l^{-1} MS salts (Sigma®), 10 ml l^{-1} MS vitamins (Murashige and Skoog 1962), 30 g l^{-1} sucrose (Sigma®) and 7 g l^{1} Agar (Isofar®), pH 5.7. The medium was poured into glass vials and autoclaved for 20 min at 121°C. The seeds were maintained in in vitro conditions until developing into seedlings, whose leaves were used for the flow cytometry procedures. After seed germination, 1.0–2.0 cm roots were used in cytogenetic procedures.

Nuclear DNA content

Nuclei extraction of *P. edulis* and *P. quadrangularis* (samples) and *S. lycopersicum* (internal standard) was performed according to Galbraith et al. (1983). Leaf fragments of 2 cm^2 were cut into Petri dishes containing 0.5 ml of OTTO I nuclear extraction buffer (Otto 1990), at 4°C, supplemented with 2 mM dithiothreitol and 50 µg ml^{-1} RNAse (Sigma®). The suspension was adjusted to 1 ml using the same buffer, filtered through a 30 µm nylon mesh (Partec®) in 1.5 ml microtube, and then centrifuged at 100 *xg* for 5 min. The supernatant was discarded and the pellet resuspended and incubated for 10 min in 100 µl of OTTO-I nuclear extraction buffer. Subsequently, the suspensions were stained for 30 min in the dark with 1.5 ml of OTTO-I:OTTO-II (1:2) staining buffer (Otto 1990), supplemented with 50 mM dithiothreitol, 50 µg ml^{-1} RNase and 75 µM of propidium iodide (Sigma®). Then, the suspensions were filtered through a nylon mesh (Partec®) of 20 µm and analyzed on a Partec PAS® flow cytometer (Partec® Gmbh, Munster, Germany) equipped with a laser source (488 nm). The histograms were analyzed in the FlowMax program (Partec® Gmbh). Mean nuclear genome sizes of *P. edulis* and *P. quadrangularis* were obtained by multiplying the 2C value of *S. lycopersicum* (internal standard) by the ratio of fluorescent intensity corresponding to the G_0/G_1 nuclei peak.

Prometaphases and metaphases

Approximately 1.0–2.0 cm roots of the in vitro germinated seeds were treated with 4 µM antitubulin amiprophos-methyl (APM, Sigma®, Carvalho et al. 2007) or with 4 µM APM/95.0 µM cycloheximide (Sigma®, Reis et al. 2014) from 1 h–8:30 h at 30ºC and roots gathered every 30 min, 16 h at 25ºC, or 16 h at 4ºC. Roots were washed with distilled water and fixed in methanol: acetic acid solution (3:1), changing this solution three times for 10 min each, and, after the last change, the material was stored at -20°C (Carvalho et al. 2007). After 24 h, the roots were washed with distilled water, and each apical root meristem was excised and transferred to 2 ml microtube containing enzymatic pool (4% cellulase – C1184 Sigma®, 1% macerozyme – R10 Kinki Yakult MFG, 0.4% hemicellulase – H2125 Sigma® diluted in pectinase E6287 – Sigma®) diluted in distilled water in a ratio of 1:40–1:60 (enzymatic pool: distilled water). Each meristem was enzymatically macerated for 2 h at 34°C, washed with distilled water to remove the enzymatic pool, fixed in methanol: acetic acid (3:1) and stored at -20ºC. After at least 12 h, slides were prepared by root meristem dissociation (one per slide) and air-drying techniques, and placed on a hot plate at 50ºC (Carvalho et al. 2007).

Immediately after preparation, all slides were evaluated on the Nikon Eclipse Ci (Nikon) phase contrast microscope and selected for ICM and fluorescence in situ hybridization (FISH) following the criteria: (a) mitotic cells with little or no cytoplasmic background, (b) chromosomes with well-defined telomere and centromere, and (c) chromosomes without overlaps and structural deformations of the chromatin.

Morphometry and chromosomal DNA content

Some pre-selected slides were stored in methanol: formaldehyde: acetic acid (17:5:1) fixative for 24 h at 25°C, washed in distilled water and submitted to the Feulgen reaction. For this, the chromosomes in the slides were hydrolyzed in 5 M HCl (Merck®) at 25ºC for 18–24 min. The slides were washed in distilled water, and stained for 12 h at 4°C with Schiff's reagent (in 100 ml: 0.5 g of basic fuchsine Sigma®, 15 ml of 1 M HCl, 2.23 g of potassium metabisulfite Sigma® and 0.703 g of activated charcoal Sigma®). Finally, the slides were washed three times in distilled water and air-dried (Carvalho et al. 2011).

A Nikon Eclipse 80i model (Nikon, Japan) microscope was calibrated and configured according to Carvalho et al. (2011). A standard micrometer slide (1,000 μm, Nikon, Japan) for the area spatial parameter was used for image system calibration and three tests were performed: stability, linearity and uniformity. The stability test consisted of measuring the gray level of a pixel to evaluate the variations of the light source of the microscope. During the capture routine, the system analysis was only conducted after stabilization time. The linearity test was performed with a set of certified neutral density filters: 0.15, 0.30, 0.40, 0.60, 0.90 and 2.50 (Edmund Industrial Optics). The uniformity test was conducted with 11 staggered density filters (Edmund Industrial Optics).

Prometaphase and metaphase images were captured using a CCD digital video camera of 8-bits gray (Nikon, Japan) coupled to a Nikon 80i microscope (Nikon, Japan) equipped with a stabilized light source, a 100x Nikon Pan Fluor oil immersion objective with 1.30 numerical aperture, a planat achromat condenser with 0.7 aperture, ND6 neutral density filter, and a 550–570 nm interference green color filter. The microscope was coupled to a Pentium Intel Core i5 (Termaltake – Asus) computer featuring the Nis – Elements 3.0 imaging software (Nikon, Japan).

We selected ten prometaphase/metaphase samples of *P. edulis* and of *P. quadrangularis* for DNA content measurement of each chromosome. For this, the mean 1C nuclear value (pg) obtained by flow cytometry, was proportionally distributed against the mean integrated optical density (IOD) values of each chromosome calculated by ICM (Carvalho et al. 2011). Chromosome morphometry was characterized for the same ten prometaphase/metaphase samples, and the class was determined as proposed by Levan et al. (1964) and reviewed by Guerra (1986).

18S rDNA and LTR retrotransposon sequences

18S rDNA probe was generated by PCR using the forward and reverse primers *F*: 5'-CTGCCAGTAGTCATATGC-3' and *R*: 5'-ATGGATCCTCGTTAAGGG-3' (Unfried et al. 1989). The probe of the *Copia* LTR-RT superfamily was generated with the primers *F*: 5'-TTCTGAGGCAGGAGAGGAAG-3' and *R*: 5'-GGCGTGCTTCTTTCTTGAAC-3'. *Copia* LTR-RT superfamily primers were designed from the complete sequence of this LTR-RT obtained from GenBank

for *P. edulis* 'MF401642' and 'CL43Contig33' (deposited at https://www.ncbi.nlm.nih.gov/nuccore/MF401642).

Genomic DNA was extracted according to Doyle and Doyle (1990) using leaves of in vitro *P. edulis* plantlets, the species with lower nuclear DNA content. DNA concentration was quantified in a spectrophotometer (NanoDrop 2000 Thermo Scientific®), and its integrity was verified by 1.0% agarose gel electrophoresis. PCR was performed from 200 ng genomic DNA, 1x buffer (GoTaq®), 0.5 µM of the primers (*F* and *R* of each sequence), 1.3 mM of each dNTP, 1.25 U of Taq DNA polymerase (GoTaq®) and 3.0 mM $MgCl_2$ and completed with distilled water to reach a final volume of 15 µl. Amplification conditions for 18S rDNA were: initial denaturation at 95°C for 5 min; 35 cycles at 95°C for 1 min, 60°C for 1 min and 72°C for 1 min 30 s; and final extension at 72°C for 5 min (Unfried et al. 1989). For the *Copia* LTR-RT superfamily, amplification conditions were: initial denaturation at 95°C for 5 min; 30 cycles at 95°C for 45 s, 58°C for 30 s, 72°C for 1 min 30 s; and final extension at 72°C for 5 min. The reactions were conducted in an Applied Biosystems Veriti™ 96-Well Thermal Cycler. PCR products were analyzed by electrophoresis in 1.0% agarose gel.

Amplification products showing ~200 bp of the *Copia* LTR-RT superfamily were purified using the Genomic Wizard® DNA Purification Kit according to the Promega Corporation protocol. Samples were sequenced by capillary electrophoresis in an ABI3730 apparatus using POP7 polymer and BigDye v3.1 by Myleus Biotechnology. Sequencing quality was verified using the free software Sequence Scanner Software (Applied Biosystems, deposited at: https://products.appliedbiosystems.com/ab/en/US/adirect/ab?Cmd=catNavigate2&catID=600583&tab=DetailInfo). Subsequently, the sequences were compared with those deposited in GenBank® through the BLASTn tool.

FISH

Some previously selected slides were stored in 70% ethanol at -20°C for at least 15 days, or in polypropylene vials only containing the slides at 37°C for at least 5 days. The procedures were performed according to Schwarzacher and Heslop-Harrison (2000) with modifications. The slides were treated in 1X phosphate buffer saline (PBS) for 5 min, 3% formalin (in 40 ml: 3.25 ml of 37% formaldehyde and 36.75

ml of 1X PBS buffer) for 15 min, 1X PBS buffer for 5 min and dehydrated in an ice col graded ethanol series (70%, 85%, 100%). 35 µL of hybridization mix containing 300 ng of the probe (18S rDNA or *Copia* LTR-RT superfamily), 50% formamide and 2X saline-sodium citrate (SSC) buffer was placed on the slide, which was covered with a HybriSlip™ plastic cover slip (Sigma®) and sealed with Rubber Cement (Elmer's). Chromosome and probe denaturation at 70ºC for 4 min and hybridization at 37ºC for 24 h were performed in the thermocycler (Loccus do Brasil). Post-hybridization stringency washes were conducted in 2 X SSC at 58°C for 25 min.

The slides were counterstained with 4', 6-diamidino-2-phenylindole (DAPI, Sigma-Aldrich®) and sealed with colorless enamel. Prometaphases and metaphases were captured by a monochromatic CCD digital video camera DS-Fi1c of 8-bits gray (Nikon, Japan) coupled to an epifluorescence Nikon microscope 80i (Nikon) microscope equipped with a 100X objective lens, UV-2E/C (DAPI) and EN GFP (18S rDNA and *Copia* LTR-RT superfamily probes) filters. Captured images were edited in Adobe® Photoshop CS4.

Results

Nuclear DNA content

The nuclei extraction and staining during the flow cytometry procedure resulted in histograms showing G_0/G_1 nuclei peaks with coefficient of variation below 5%. So, the mean nuclear DNA content of *P. edulis* was 2C = 3.39 ± 0.04 pg (1C = 1.695 pg) and *P. quadrangularis* was 2C = 5.46 ± 0.02 pg (1C = 2.73 pg), presenting an interspecific variation in nuclear genome size of ~61.06%. Because of this confirmed difference in 1C value, we performed the following steps: chromosome number determining, morphometric characterization, chromosomal DNA content menasurement, 18S rDNA site mapping, and *Copia* LTR-RT superfamily localization and distribution.

Prometaphases and metaphases

Taking into account the criteria used to choose the slides, the treatments that generated the highest index of prometaphase/metaphase were the 4 µM APM for 1 h 40 min at 30°C for *P. edulis* and 16 h at 4°C for *P. quadrangularis* (Fig. 1). From the obtained slides, ICM and FISH were performed from at least 10 prometaphase/metaphase samples of *P. edulis* and of *P. quadrangularis* for each application.

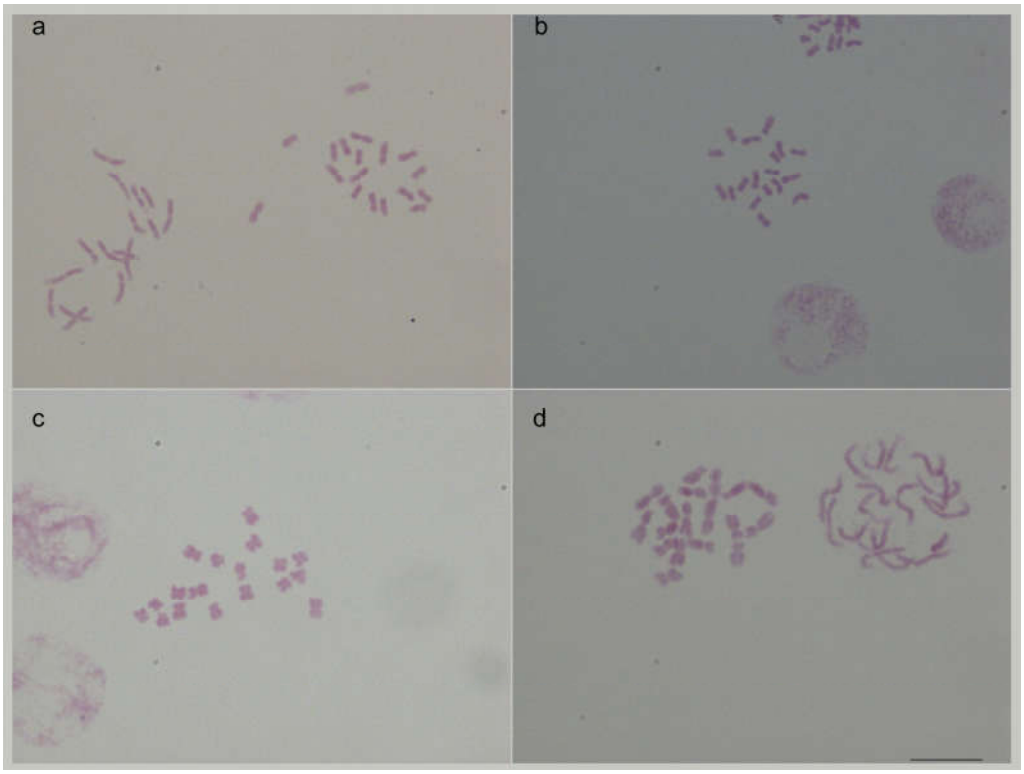

Fig. 1 – Cytogenetic preparations of *P. edulis* **(a, b)** and *P. quadrangularis* **(c, d)** presenting 2n = 18 chromosomes and showing different chromatin condensation levels. **(a)** Initial prometaphase and late prometaphase, **(b)** late prometaphase, **(c)** metaphase, **(d)** late prometaphase and prophase. Bar = 5 µm.

Morphometry and chromosomal DNA content

All chromosomes of *P. edulis* and *P. quadrangularis* were stoichiometrically stained by Feulgen reaction from hydrolysis in 5 M HCl at 25°C for 20 min in *P. edulis* (Figs. 1a, b, 2a) and for 22 min in *P. quadrangularis* chromosomes (Figs. 1c, d, 2b), and staining with Schiff's reagent for 12 h. Based on IOD values and 1C nuclear value, the mean DNA content of each chromosome was measured for ten metaphase/prometaphase samples of each *Passiflora* species. From these preparations, the morphometric characterization (total and arm lengths, and centromeric index) was also performed.

Mean total length of the *P. edulis* chromosomes ranged from 1.92 ± 0.24 µm (chromosome 1) to 1.19 ± 0.12 µm (chromosome 9). The karyogram of this species was composed of six metacentric (1, 3, 5 – 7 and 9) and three submetacentric pairs (2, 4 and 8) (Table 1, Fig. 2a). In *P. quadrangularis*, the mean total length ranged from 2.06 ± 0.46 µm (chromosome 1) to 1.28 ± 0.29 µm (chromosome 9), with two metacentric (4 and 8) and seven submetacentric pairs (1 – 3, 5 – 7 and 9) (Table 1, Fig. 2b). Concerning the morphological shapes, only chromosome 2 was classified as submetacentric in both species. The other chromosomes were classified as belonging to different classes in *P. edulis* and *P. quadrangularis* (Table 1).

Mean chromosomal DNA content values ranged from 1C = 0.2274 ± 0.0143 pg (chromosome 1) to 1C = 0.1412 ± 0097 pg (chromosome 9) in *P. edulis*, highlighting that chromosomes 2 (1C = 0.2308 ± 0.0152 pg) and 6 (1C = 0.1863 ± 0.0123 pg) presented higher mean values when compared to chromosomes 1 and 5 (1C = 0.1794 ± 0.0112 pg), respectively. In *P. quadrangularis*, the mean values varied from 1C = 0.3759 ± 0.0195 pg (chromosome 1) to 0.2177 ± 0.0241 pg (chromosome 9). Here, chromosome 8 showed a higher DNA content (1C = 0.2710 ± 0.0121 pg) than chromosome 7 (1C = 0.2592 ± 0.0149 pg).

Table 1 Mean 1C chromosomal DNA content, morphometry and chromosome class of *P. edulis* and *P. quadrangularis*.

	P. edulis							*P. quadrangularis*						
Chromosome	1C (pg)	% Size*	Total (µm)	% Size**	Arms (µm)		Class	1C (pg)	% Size*	Total (µm)	% Size**	Arms (µm)		Class
					Short	Long						Short	Long	
1	0.2274 ± 0.0143	13.42	1.92 ± 0.24	13.67	0.81	1.11	M	0.3759 ± 0.0195	13.77	2.06 ± 0.46	13.74	0.70	1.36	SM
2	0.2308 ± 0.0152	13.62	1.89 ± 0.21	13.49	0.68	1.22	SM	0.3538 ± 0.0168	12.96	1.94 ± 0.43	12.92	0.77	1.17	SM
3	0.2124 ± 0.0147	12.53	1.75 ± 0.22	12.47	0.75	1.00	M	0.3450 ± 0.0185	12.64	1.89 ± 0.42	12.58	0.71	1.18	SM
4	0.1943 ± 0.0159	11.46	1.60 ± 0.19	11.40	0.60	1.00	SM	0.3161 ± 0.0165	11.58	1.80 ± 0.34	11.98	0.80	1.00	M
5	0.1794 ± 0.0112	10.58	1.54 ± 0.19	10.98	0.65	0.89	M	0.3085 ± 0.0184	11.30	1.58 ± 0.30	10.52	0.62	0.96	SM
6	0.1863 ± 0.0123	10.99	1.48 ± 0.19	10.55	0.63	0.85	M	0.2829 ± 0.0085	10.36	1.56 ± 0.30	10.35	0.62	0.94	SM
7	0.1677 ± 0.0073	9.89	1.38 ± 0.13	9.84	0.59	0.79	M	0.2592 ± 0.0149	9.49	1.49 ± 0.32	9.91	0.53	0.96	SM
8	0.1556 ± 0.0109	9.18	1.28 ± 0.14	9.12	0.48	0.81	SM	0.2710 ± 0.0121	9.93	1.43 ± 0.34	9.49	0.58	0.85	M
9	0.1412 ± 0.0097	8.33	1.19 ± 0.12	8.48	0.49	0.70	M	0.2177 ± 0.0241	7.97	1.28 ± 0.29	8.54	0.40	0.88	SM
Total	1.695	100.00	14.03	100.00				2.73	100.00	15.02	100.00			

1C – mean 1C chromosomal DNA content in pg (± SD); mean total (± SD), short and long arms in µm; size – % size in relation to sum of the mean 1C value* and total length**; M – metacentric; SM – submetacentric.

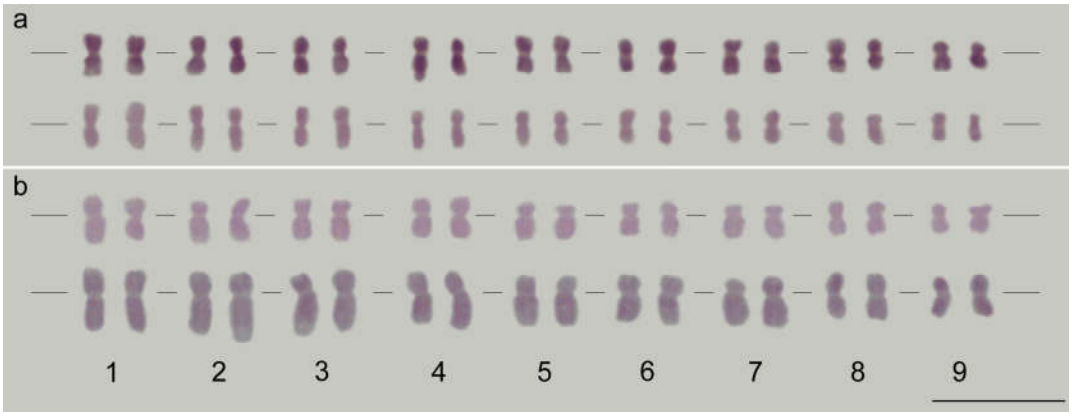

Fig. 2 – *P. edulis* **(a)** and *P. quadrangularis* **(b)** karyograms showing chromosomes stoichiometrically stained with Schiff's reagent. **(a)** *P. edulis* and **(b)** *P. quadrangularis* karyograms displaying higher (above) and lower (below) chromatin compaction level. In *P. edulis*, the chromosomes 1, 3, 5 – 7 and 9 are metacentrics, and 2, 4 and 8 are submetacentrics. Chromosomes 2 and 6 showed higher DNA content than chromosomes 1 and 5, respectively. In *P. quadrangularis*, chromosomes 4 and 8 are metacentrics, and 1 – 3, 5 – 7 and 9 are submetacentrics. Chromosome 8 had more DNA content than chromosome 7. Bar = 5 μm.

18S rDNA and LTR retrotransposon sequences

The *F* primer for the *Copia* LTR-RT superfamily sequence generated an amplification product with 213 pb, and the product generated by the *R* primer presented 207 pb. BLASTn analysis showed high homology between the amplified and the database sequences, specifically 87% for the *F* primer and 94% for the *R* primer.

18S rDNA site was reproductively visualized in 25 prometaphase/metaphase samples of *P. edulis*, and mapped on the terminal portion of the long arm on chromosome 6 and the terminal portion of the short arm on chromosome 8 (Fig. 3a). In *P. quadrangularis*, 18S rDNA site was mapped in 19 prometaphase/metaphase samples. In 15 prometaphase/metaphase samples, 18S rDNA was located in the terminal portion of the chromosome 7 long arm. In 4 prometaphase/metaphase samples, 18S rDNA was also mapped on the terminal portion of the chromosome 8 short arm (Fig. 3b). Cytological features in each prometaphase/metaphase sample, even on the same slide, resulted in the distinct number of 18S

rDNA sites in *P. quadrangularis*. Cytoplasmic debris, which were identified through background comparisons, promoted a physical barrier, probably blocking the 18S rDNA probe from the target DNA in chromosome 8. So, we concluded that *P. quadrangularis* possesses two chromosomes with an 18S rDNA site.

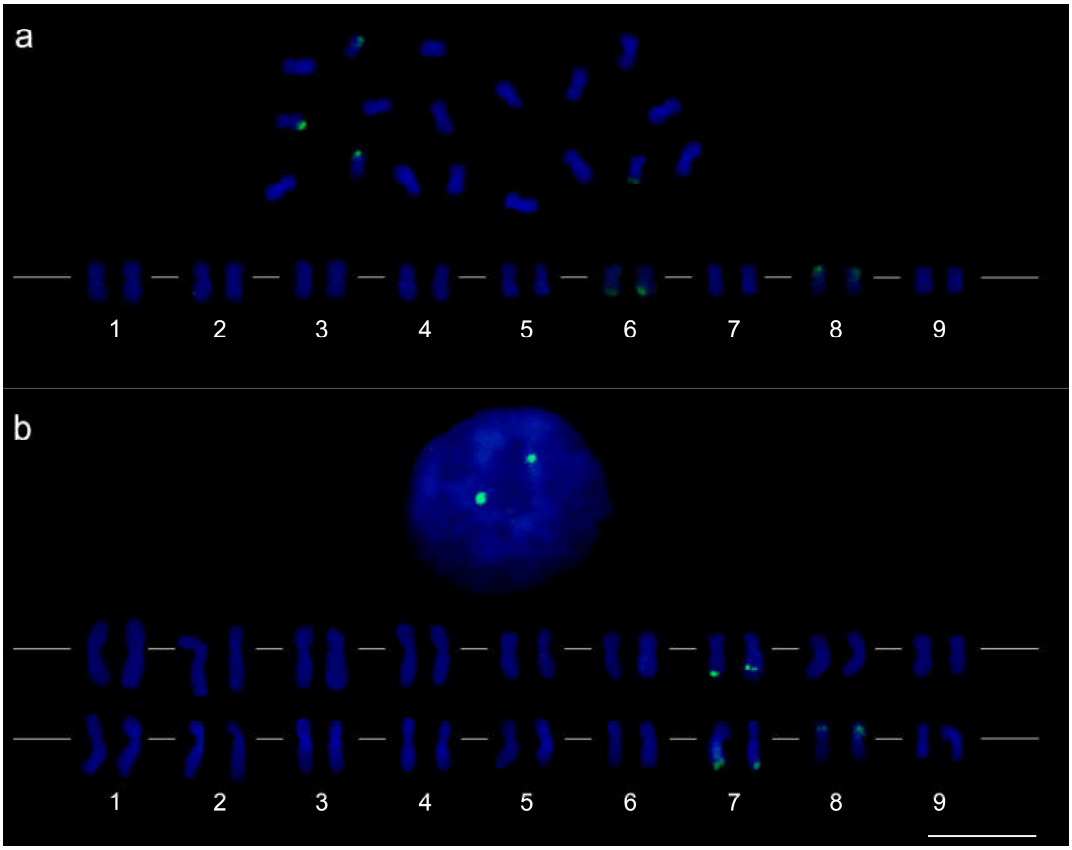

Fig. 3 – FISH in *P. edulis* metaphase chromosomes **(a)**, and in interphase nucleus and prometaphase chromosomes of *P. quadrangularis* **(b)** with 18S rDNA probe labelled with ChromaTide-488-5-dUTP (green) counterstained with DAPI. **(a)** *P. edulis* 18S rDNA sites were mapped on the terminal portion of the chromosome 6 long arm and in the terminal portion of the chromosome 8 short arm. **(b)** *P. quadrangularis* 18S rDNA signal was identified in the interphase nucleus and in below karyogram at the terminal portion of the chromosome 7 long arm. Two 18S rDNA sites were mapped at the terminal portion of the chromosome 7 long arm and the terminal portion of the chromosome 8 short arm (last karyogram). Bar = 5 µm.

Dispersed hybridization signals from the *Copia* LTR-RT superfamily probe were observed in 30 prometaphase/metaphase samples of *P. edulis.* Stronger signals were found on chromosomes 3, 4 and 6, and weaker signals on chromosomes 1, 2, 5, and 7 – 9. The hybridization signal on chromosome 2 was predominant in the short arm portion, and on chromosome 8, the hybridization signal was stronger on one of the homologous pairs. In general, the signals were dispersed throughout the length of the chromosomes (Fig. 4a). In *P. quadrangularis*, dispersed hybridization signals were found in 20 karyotypes. Intense hybridization signals were observed on chromosomes 1, 4, 5 and 8, and weaker hybridization signals on chromosomes 2, 3, 6, 7 and 9. Chromosomes 7 and 9 accumulated weaker signals in the interstitial portions at the long arms (Fig. 4b). In both species, chromosome 4 exhibited stronger signals, while chromosome 9 showed weaker signals. In general, the hybridization signals were more accumulated in *P. quadrangularis* than in *P. edulis* chromosomes (Fig. 4).

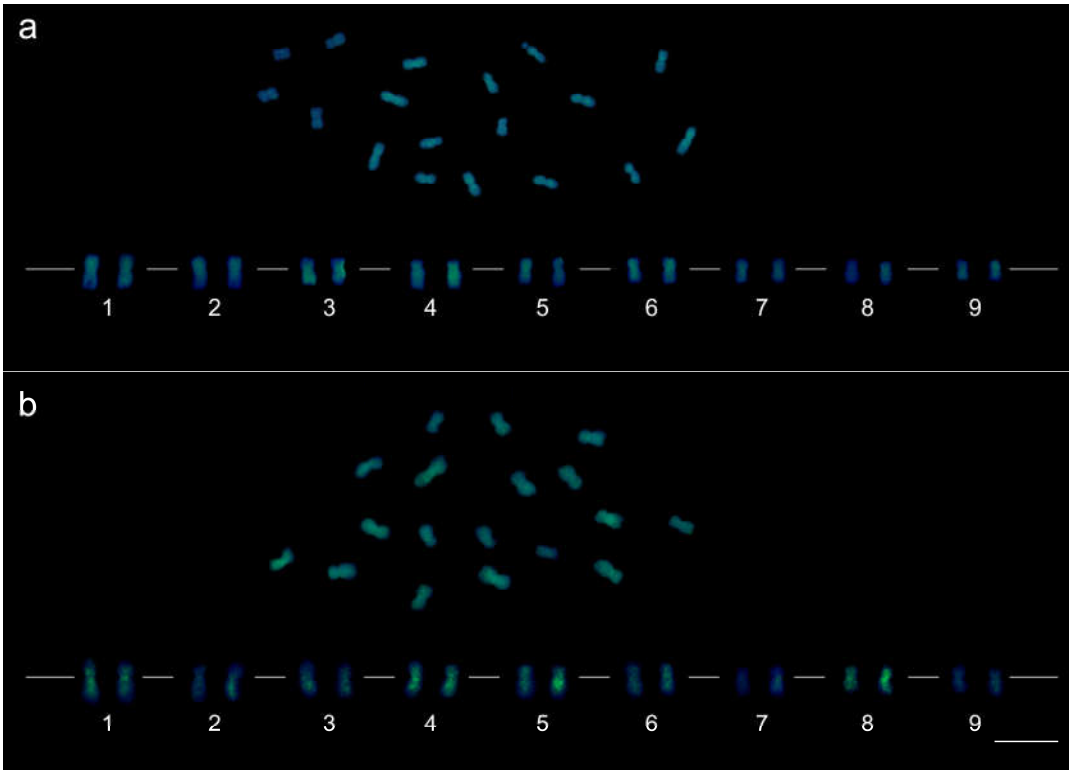

Fig. 4 – FISH in metaphase chromosomes stained with DAPI (blue) and *Copia* LTR-RT superfamily probe labelled with ChromaTide-488-5-dUTP (green), along *P. edulis* **(a)** and *P. quadrangularis* **(b)** chromosomes. FISH produced more scattered and accumulated hybridization signals in some chromosomes than in others. **(a)** In *P. edulis* prometaphases/metaphases, the hybridization signals were

dispersed and stronger on chromosomes 3, 4 and 6, and weaker on the other chromosomes. **(b)** In *P. quadrangularis* chromosomes, the stronger signals were observed on chromosomes 1, 4, 5 and 8, and weaker signals on the other chromosomes. It is noteworthy that in both species the chromosome 4 presented stronger hybridization signals, and chromosome 9 presented weaker signals. In addition, the signals were stronger on the *P. quadrangularis* chromosomes than *P. edulis*. Bar = 5 µm.

Discussion

Copia LTR-RT superfamily promotes the nuclear DNA content variation

Even though LTR-RT is the most abundant class of transposable elements in plants, the process through which LTR-RT have shaped plant genomes in different ways is still poorly understood. In this study, we aimed to understand the role of the *Copia* LTR-RT superfamily in genome size variation between two *Passiflora* species, which possess the same 2n chromosome number but different 2C DNA values. Our results show that the occurrence of the *Copia* LTR-RT superfamily in the chromosomes of *P. edulis* and *P. quadrangularis* is a relevant cause for the nuclear 2C value variation of ~61.06%. Transposable elements (TEs) accounted for 17.6% of 10.4 Mb of the sequenced genome (~1% of the total genome size) from 112 bacterial artificial chromosome (BAC) inserts from the *P. edulis* genomic library (Munhoz et al. 2018). According to these authors, these TEs were preferentially hosted in intergenic regions. The LTR-RT was the most frequent, and accounted for 75.1% of retrotransposons, corresponding to 1,418,389 bp or 13.6% (1,418,389 bp/10,401,671 bp) of all sequenced data. In another sequencing approach, it was unraveled that the *P. edulis* genome shows 19.6% of repetitive DNA sequences, 18.5% (~1.14 Mb) of which represented by LTR-RT (Santos et al. 2014). Based on the 1C = 1.695 pg (1C = 1.65771 Gb) value measured here and published sequenced genome data (Santos et al. 2014; Munhoz et al. 2018), LTR-RT are equivalent to ~0.07% of the *P. edulis* genome. The abundance in LTR-RT is very similar in the two previous *Passiflora* genome reports (Santos et al. 2014; Munhoz et al. 2018). However, our FISH data indicate that the proportion of the *Copia* LTR-RT superfamily is higher. Probably, these species have a large proportion of LTR-RT, as is also observable in other species: *Z. mays* with 75%

(Schnable et al. 2009), *S. lycopersicum* with 62% (Paz et al. 2017) or *A. thaliana* where 20% of the genome are comprised of retrotransposons (Underwood et al. 2017). On the other hand, Munhoz et al. (2018) stated that the content of LTR elements in *P. edulis* is comparable to that identified in related Malpighiaceae species, such as *Populus trichocarpa* (~25% LTR-TR), *Ricinus communis* (~16% LTR-RT) and *Manihot esculenta* (~11% LTR-RT), although they recognized the highly variable abundance of these sequences, which is evidence for the importance of transposable elements in genome evolution.

Although LTR-RT has been previously reported only for *P. edulis* (Santos et al. 2014; Munhoz et al. 2018), it was presumed that *P. quadrangularis* must have these elements because of the "ancestral library" hypothesis (Salser et al. 1976). This hypothesis proposes that phylogenetically related species share an "ancestral library" containing several repetitive DNA sequences conserved over evolutionary periods (Salser et al. 1976). In addition, the two species derived from a common ancestor with a divergence time of ~16.8 millions of years ago (Muschner et al. 2012).

Several authors have emphasized the importance of transposable elements in plant genome size variation. Taking into account the replication mechanism of LTR-RT, the higher 1C value and higher number of *Copia* LTR-RT superfamily hybridization signals observed in *P. quadrangularis* compared to *P. edulis* can be explained as an outcome of the balancing between accumulation (retrotransposition) and elimination (unequal homologous recombination and/or illegitimate recombination) events throughout the evolution of the species. These processes are random during karyotype evolution and may be uncorrelated with phylogenetic placement (Grover et al. 2008). Considering that the phylogeny of the *Passiflora* genus (proposed by Muschner et al. 2003) showed *P. edulis* to be more basal than *P. quadrangularis*, the higher DNA content as well as higher number of LTR-RT signals (Figs. 2, 4 and 5) found in *P. quadrangularis* can be explained by an increased genome size due to the accumulation/amplification of retrotransposable elements. In accordance with our results, genome size increase promoted by retrotransposition, involving the amplification of new LTR-RT copies and their transpositions, was observed in *Z. mays* (Schnable et al. 2009) and *S. lycopersicum* (Paz et al. 2017). In contrast, the genome size can decrease by LTR-RT removal through unequal homologous recombination and/or illegitimate recombination, as reported in *A. thaliana* (Bennetzen et al. 2005) and *Oryza sativa L.* (Vitte et al. 2007). Moreover, *Copia* LTR-RT superfamily contribution to nuclear genome size variation was observed in *Helianthus* L. species with the same chromosome number. *Helianthus petiolaris* ssp. Fallax showed 1C = 5.78 pg and *Helianthus*

agrestis Pollard 1C = 16.24 pg, both with 2n = 34 chromosomes. Corroborating these results, the LTR-RT content ranged from 73.6% in *H. petiolaris* to 84.2% in *H. agrestis*. So, the interspecific nuclear DNA variation was attributed to the occurrence and abundance of *Copia* and *Gypsy* LTR-RT superfamilies (Mascagni et al. 2017).

Looking for influence of the Copia LTR-RT superfamily on Passiflora karyotype evolution

Cytogenetic results confirmed the monophyletic origin of *P. edulis* and *P. quadrangularis*. Similarly, divergences promoted by the *Copia* LTR-RT superfamily were also observed in each chromosome of the two species. So, cytogenetic preparations of mitotic cells with little or no cytoplasmic background, as well as chromosomes with well-defined telomere and centromere, without overlaps and structural chromatin deformations are fundamental, which is why tiny adjustments in the cytogenetic protocol are usually necessary. Among the similarities found in the karyotypes, especially the chromosome number 2n = 18, the occurrence of only metacentric and submetacentric chromosomes, the number of 18S rDNA sites, and 18S rDNA localization in the terminal portion of the chromosome 8 short arm should be highlighted. In contrast, divergences between the species were observed when each chromosome was qualitatively (through morphometry, 18S rDNA localization and LTR-RT signals) and quantitatively (chromosomal DNA content) characterized and compared (Table 1, Figs. 2, 3, 4 and 5).

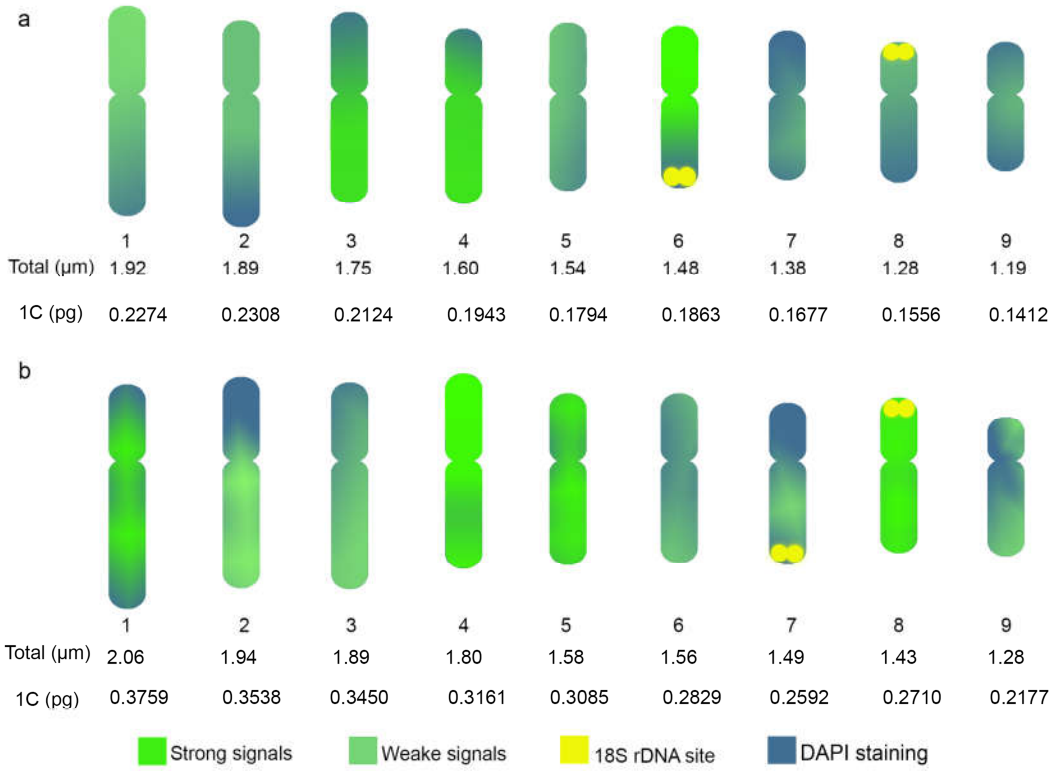

Fig. 5 – Ideogram of *P. edulis* **(a)** and *P. quadrangularis* **(b)** summarizing the data about total length (µm), chromosome class, mean 1C chromosomal DNA content value (pg), stronger and weaker signals from the *Copia* LTR-RT superfamily and 18S rDNA mapping.

Nuclear genome size variation between *P. edulis* and *P. quadrangularis* is differently and randomly distributed among all the chromosomes of the karyotypes. We found that some chromosomes stood out with higher DNA content and more *Copia* LTR-RT superfamily hybridization signals than others (Table 1, Fig. 5). Comparing the chromosomes individually (e.g. chromosome 1 of *P. edulis* to chromosome 1 of *P. quadrangularis*, Fig. 5), *P. edulis* chromosomes showed smaller mean total lengths, lower DNA contents and weaker *Copia* LTR-RT superfamily signals compared to respective *P. quadrangularis* chromosomes. These data corroborate with a larger nuclear genome size in *P. quadrangularis*.

P. edulis chromosome 6 and *P. quadrangularis* chromosome 7 presented an 18S rDNA site in the same portion (Figs. 4 and 5), thus these chromosomes were unequivocally identified by this marker.

Considering that the species are monophyletic taxa (Muschner et al. 2003, 2012), the karyotypes of these species underwent modifications that promoted differences in the mean total and arm length, chromosomal class (Table 1, Figs. 3, 4 and 5) and DNA content (Table 1, Fig. 5). Such changes were so accentuated that *P. edulis* chromosome 6 and in *P. quadrangularis* chromosome 7 are positioned differently in the karyograms according to chromosome classification rules (Levan et al. 1964; Guerra 1986). Corroboratingly, chromosome 8 of both species showed the same 18S rDNA mapping (Figs. 4 and 5), thus probably the same ancestral chromosome. The observed changes in chromosome 8 in each species also caused divergences in the classification using the morphometry (Table 1) and DNA content data. These alterations also involved the *Copia* LTR-RT superfamily, which is more predominant in *P. quadrangularis'* chromosome 8 (Fig. 5). The occurrence and distribution of the *Copia* LTR-RT superfamily between the *P. edulis* and *P. quadrangularis* chromosomes suggest that the differences could be due to accumulation/elimination of these sequences, leading to an increase/decrease of the DNA content, culminating in chromosome morphometry modifications.

Copia LTR-RT superfamily hybridization signals were predominantly distributed from telomere to telomere of the *P. edulis* and *P. quadrangularis* chromosomes (Figs. 4 and 5). The distribution of the *Copia* LTR-RT superfamily can be dispersed throughout the extension in plant chromosomes, occurring in euchromatic regions and in higher copy number in heterochromatic regions (Contreras et al. 2015). However, as natural selection tends to eliminate deleterious insertions, there is a greater concentration of retrotransposons insertions in gene-poor regions, such as the heterochromatic repetitive regions (Graham and Boissinot 2006; Zamudio et al. 2015). According to Munhoz et al. (2018), 70.4% of transposable elements identified in the sequenced genome of *P. edulis* were preferentially hosted in intergenic regions. This data is in accordance with the spread distribution of the *Copia* LTR-RT superfamily found in this study. Additionally, LTR-RT distribution in different chromatin regions has also been described for other taxa. In *A. thaliana*, the pericentromeric heterochromatin has expanded 6 to 10 times in the last 5 million years due to the retrotransposition (Hall et al. 2006). In *Z. mays* (Mroczek and Dawe 2003) and in *S. lycopersicum* (Xu and Du 2014), the *Copia* LTR-RT superfamily has been diffused by euchromatin. LTR-RT also occur in heterochromatin of the telomeric regions in *E. arundinaceus* (Huang et al. 2017), and centromeric and pericentromeric regions in *Coffea* (Castro Nunes et al. 2018).

Total chromosome length, chromosomal DNA content and LTR retrotransposons: understanding intraspecific karyotype variations

Intraspecifically, there is no relation between the total length and DNA content for some chromosomes: chromosomes 2 and 6 in *P. edulis*, and chromosome 8 in *P. quadrangularis* have a relative lower total length but higher DNA content (Table 1, Figs. 2, 3, 4 and 5). Looking at each *Passiflora* species allowed us to analyze the role of the *Copia* LTR-RT superfamily in the karyotype evolution.

In the *P. edulis* karyotype, chromosome 2 presented a lower total length and a higher DNA content than chromosome 1 (Table 1, Fig. 5). This suggests that the chromatin condensation level of chromosome 2 is higher than of chromosome 1. *Copia* LTR-RT superfamily hybridization signals were weaker and more dispersed from telomere to telomere in chromosome 1, while chromosome 2 showed stronger signals predominantly in the long arm (Table 1, Figs. 4 and 5). Therefore, other types of repetitive DNA sequence might be present on chromosome 2, such as simple repeats and elements of low complexity that represent about to 1% (0.0028 Mb) of transposable elements identified in *P. edulis* BES (Santos et al. 2014). *P. edulis'* chromosome 6 had a lower total length and a greater amount of *Copia* LTR-RT superfamily signals compared to chromosome 5 (Table 1, Figs. 4 and 5), evidencing that the increased DNA content on chromosome 6 and the relatively larger chromatin condensation level is promoted by the accumulation of LTR-RT sequences. The same was observed in *P. quadrangularis'* chromosome 8 that presented a smaller total length, and a higher DNA content, more *Copia* LTR-RT superfamily signals and a higher compaction level than chromosome 7 (Table 1, Fig. 5). These retroelements are mainly found in heterochromatic regions (Bennetzen 2000; Gao et al. 2008; Bierhoff et al. 2013; Li et al. 2017) and, thus, the *Copia* LTR-RT superfamily hybridization signals can be related to these portions. Heterochromatin has a higher chromatin condensation level than euchromatin (Bennetzen 2000). Therefore, a higher condensation level results in a smaller total length, despite a higher DNA content in these chromosomes.

As observed in *Z. mays* 'AL Bandeirante', the DNA content, accessed by ICM, of chromosome 9 (1C = 0.280 pg) is higher than of chromosome 8 (1C = 0.266 pg, Silva et al. 2018). This difference was related to differential DAPI staining that evidenced a knob portion in the long arm of the chromosome 9. So, Silva et al. (2018) suggested that the chromosomal DNA content variation between these two *Z. mays* chromosomes was promoted by occurrence of the heterochromatin in the knob. The retrotransposons

occur in abundance in this region, and due to this the activity of these elements can play an important role in the alteration in the DNA content observed in *Z. mays* (Silva et al. 2018). In the two *Passiflora* species analyzed, the chromosomes have different amounts of LTR-RT, which account for differences in DNA content, chromatin compaction level, and consequently the chromosome's total length. Nevertheless, the ICM technique allowed inter- and intraspecifically to discriminate each chromosome, showing tiny DNA content differences between them.

Conclusions

Our findings showed that the *Copia* LTR-RT superfamily promotes nuclear and chromosomal DNA content variations between *P. edulis* and *P. quadrangularis*, with DNA content and retroelements being distributed differently and randomly in the chromosomes. By analyzing each chromosome from qualitative and quantitative characterization, it was possible to identify some causes of the karyotype evolution and the actual structural organization of the chromosomes of *P. edulis* and *P. quadrangularis*.

Acknowledgments

We would like to thank the Conselho Nacional de Desenvolvimento Científico e Tecnológico (CNPq, Brasília – DF, Brazil, grants 443801/2014-2, 448671/2014-0 and 308828/2015-1) and Fundação de Amparo à Pesquisa do Espírito Santo (FAPES, Vitória – ES, Brazil, grants 65942604/2014 and 0438/2015) for financial support. This study was also financid in part by the Coordernação de Aperfeiçoamento de Pessoal de Nível Superior -Brasil (CAPES) – Finance Code 001.

Compliance with ethical standards

Conflict of interest: The authors declare that they have no conflict of interest.

Ethical approval: This article does not contain any studies with human participants or animals performed by any of the authors

Author contribution statement: The authors Vieira AT, Mendonça MAC and Clarindo WR conceived, designed and conducted the tissue culture, cytogenetic and image cytometry approaches. The authors Vieira AT and Clarindo WR performed the flow cytometry analysis. Vieira AT, Soares FAF and Leite CT performed fluorescent in situ hybridization. Vieira AT, Clarindo WR and Mendonça MAC wrote, edited and reviewed the manuscript. All authors approved the final manuscript submission version.

References

Bennetzen JL (2000) The many hues of plant heterochromatin. Genome Biol 1:107-1. https://doi.org/10.1186/gb-2000-1-1-reviews107

Bennetzen JL, Ma J, Devos KM (2005) Mechanisms of recent genome size variation in flowering plants. Ann Bot 95:127-132. https://doi.org/10.1093/aob/mci008

Bennetzen JL, Wang H (2014) The contributions of transposable elements to the structure, function, and evolution of plant genomes. Annu Rev Biol 65:505-530. https://doi.org/10.1146/annurev-arplant-050213-035811

Bierhoff H, Postepska-Igielska A, Grummt I (2014) Noisy silence: non-coding RNA and heterochromatin formation at repetitive elements. Epigenetics 9:53-61. https://doi.org/10.4161/epi.26485

Bogunic F, Muratovic E, Brown SC, Siljak-Yakovlev S (2003) Genome size and base composition of five *Pinus* species from the Balkan region. Plant Cell Rep 22:59–63. http://doi.org/10.1007/s00299-003-0653-2

Carvalho CR, Clarindo WR, Almeida PM (2007) Plant cytogenetics: still looking for the perfect mitotic chromosomes. Nucleus 50:453–462.

Carvalho CR, Clarindo, WR, Abreu, IS (2011) Image cytometry: nuclear and chromosomal DNA quantification. Methods Mol Biol 689:51-68. http://doi.org/10.1007/978-1-60761-950-5_4

Castro Nunes R, Orozco-Arias S, Crouzillat D, Mueller LA, Strickler SR, Descombes P ... Vanzela AL (2018) Structure and distribution of centromeric retrotransposons at diploid and allotetraploid *Coffea* centromeric and pericentromeric regions. Front Plant Sci 9:175. https://doi.org/10.3389/fpls.2018.00175

Chang SB, Yang TJ, Datema E, van Vugt J, Vosman B, Kuipers A, ... de Jong H (2008) FISH mapping and molecular organization of the major repetitive sequences of tomato. Chromosome Res 16:919-933. https://doi.org/10.1007/s10577-008-1249-z

Contreras B., Vives C., Castells R., Casacuberta J.M. (2015) The Impact of Transposable Elements in the Evolution of Plant Genomes: From Selfish Elements to Key Players. In: Pontarotti P. (eds) Evolutionary Biology: Biodiversification from Genotype to Phenotype. Springer, Cham. https://doi.org/10.1007/978-3-319-19932-0_6

Díez CM, Gaut BS, Meca E, Scheinvar E, Montes-Hernandez S, Eguiarte LE, Tenaillon MI (2013) Genome size variation in wild and cultivated maize along altitudinal gradients. New Phytol 199:264-276. https://doi.org/10.1111/nph.12247

Doyle JJ, Doyle JL (1990) Isolation of plant DNA from fresh tissue. Focus 12:13-15. https://doi.org/10.4236/ajps.2017.86079

Eickbush TH, Jamburuthugoda, VK (2008) The diversity of retrotransposons and the properties of their reverse transcriptases. Virus Res 134:221-234. https://doi.org/10.1016/j.virusres.2007.12.010

Freeling M, Xu J, Woodhouse M, Lisch D (2015) A solution to the C-value paradox and the function of junk DNA: the genome balance hypothesis. Mol Plant 8:899-910. https://doi.org/ 10.1016/j.molp.2015.02.009

Galbraith DW, Harkins KR, Maddox JM, Ayres NM, Sharma DP, Firoozabady E (1983) Rapid flow cytometric analysis of the cell cycle in intact plant tissues. Science 220:1049-1051. https://doi.org/10.1126/science.220.4601.1049

Gao X, Hou Y, Ebina H, Levin HL, Voytas DF (2008) Chromodomains direct integration of retrotransposons to heterochromatin. Genome Res 18:359-369. https://doi.org/10.1101/gr.7146408

Graham T, Boissinot S (2006) The genomic distribution of L1 elements: the role of insertion bias and natural selection. J Biomed Biotechnol 1:1-5. https://doi.org/10.1155/JBB/2006/75327

Grover C E, Hawkins JS, Wendel JF (2008) Phylogenetic insights into the pace and pattern of plant genome size evolution. Genome Dyn 4:57-68. https://doi.org/10.1159/000126006

Guerra MS (1986) Reviewing the chromosome nomenclature of Levan et al. Braz J Genet 9:741-743

Hall AE, Kettler GC, Preuss D (2006) Dynamic evolution at pericentromeres. Genome Res 16:355-364. https://doi.org/10.1101/gr.4399206

Hansen AK, Lawrence G, Simpson BB, Downie SR, Stephen R, Cervi AC, Jansen RK (2006) Phylogenetic relationships and chromosome number evolution in *Passiflora*. Syst Bot 31:138–150. https://doi.org/ 10.1600/036364406775971769

Huang Y, Luo L, Hu X, Yu F, Yang Y, Deng Z, ... Zhang M (2017) Characterization, genomic organization, abundance, and chromosomal distribution of Ty1-copia Retrotransposons in *Erianthus arundinaceus*. Front Plant Sci 8:924. https://doi.org/10.3389/fpls.2017.00924

Levan A, Fredga K, Sandberg AA (1964) Nomenclature for centromeric position on chromosomes. Hereditas 52: 201-220. https://doi.org/10.1111/j.1601-5223.1964.tb01953.x

Li SF, Su T, Cheng GQ, Wang BX, Li X, Deng CL, Gao WJ (2017) Chromosome evolution in connection with repetitive sequences and epigenetics in plants. Genes 8:290. https://doi.org/10.3390/genes8100290

Mascagni F, Giordani T, Ceccarelli M, Cavallini A, Natali L (2017) Genome-wide analysis of LTR-retrotransposon diversity and its impact on the evolution of the genus *Helianthus* (L.). BMC Genomics 18:634. https://doi.org/10.1186/s12864-017-4050-6

Mroczek RJ, Dawe RK (2003) Distribution of retroelements in centromeres and neocentromeres of maize. Genetics 165:809-819.

Munhoz CF, Costa ZP, Cauz-Santos LA, Reátegui ACE, Rodde N, Cauet S, Dornelas MC, Leroy P, Varani AM, Bergès H, Vieira MLC (2018) A gene-rich fraction analysis of the *Passiflora edulis* genome reveals highly conserved microsyntenic regions with two related Malpighiales species. Sci Rep 8: 13024. https://doi.org/10.1038/s41598-018-31330-8

Murashige T, Skoog F (1962) A revised medium for rapid growth and bio assays with tobacco tissue cultures. Physiol Plant 15:473-497. https://doi.org/10.1111/j.1399-3054.1962.tb08052.x

Muschner VC, Lorenz AP, Cervi AC, Bonatto SL, Souza-Chies TT, Salzano FM, Freitas LB (2003) A first molecular phylogenetic analysis of *Passiflora* (Passifloraceae). Am J Bot 90:1229-1238. https://doi.org/10.3732/ajb.90.8.1229

Muschner VC, Zamberlan PM, Bonatto SL, Freitas LB (2012) Phylogeny, biogeography and divergence times in *Passiflora* (Passifloraceae). Genet Mol Biol 35:1036-1043

Otto F (1990) DAPI staining of fixed cells for high-resolution flow cytometry of nuclear DNA. In: Darzynkiewiez Z, Crissman HA, Robinson JP (Eds). Methods Cell Biol 33:105-110

Paz RC, Kozaczek, ME, Rosli HG, Andino NP, Sanchez-Puerta MV (2017) Diversity, distribution and dynamics of full-length *Copia* and *Gypsy* LTR retroelements in *Solanum lycopersicum*. Genetica 145:417-430. https://doi.org/10.1007/s10709-017-9977-7

Praça-Fontes MM, Carvalho CR, Clarindo WR (2011) C-value reassessment of plant standards: an image cytometry approach. Plant Cell Rep 30:2303-2312. https://doi.org/10.1007/s00299-011-1135-6

Rosado TB, Clarindo WR, Carvalho CR (2009) An integrated cytogenetic, flow and image cytometry procedure used to measure the DNA content of *Zea mays* A and B chromosomes. Plant Sci 176:154-158. https://doi.org/10.1016/j.plantsci.2008.10.007

Salser W, Bowen S, Browne D, El-Adli F, Fedoroff N, Fry K, ... Whitcome P (1976) Investigation of the organization of mammalian chromosomes at the DNA sequence level. Fed Proc 35:23-35

Santos AA, Penha HA, Bellec A, de Freitas Munhoz C, Pedrosa-Harand A, Bergès H, Vieira MLC (2014) Begin at the beginning: A BAC-end view of the passion fruit (*Passiflora*) genome. BMC Genomics 15:816. https://doi.org/10.1186/1471-2164-15-816

Schnable PS, Ware D, Fulton RS, Stein JC, Wei F, Pasternak S... Minx P (2009) The B73 maize genome: complexity, diversity, and dynamics. Science 326:1112-1115. https://doi.org/10.1126/science.1178534

Schwarzacher T, Heslop-Harrison JS (2000) Practical in situ hybridisation. 1st edn. 203 pp. Oxford: Bios Scientific Publishers. £21.95 (softback). Ann Bot 86:433-433. https://doi.org/10.1006/anbo.2000.1169

Silva JC, Carvalho CR, Clarindo WR (2018) Updating the maize karyotype by chromosome DNA sizing. PloS ONE 13:e0190428. https://doi.org/ 10.1371/journal.pone.0190428

Souza MM, Pereira TNS, Carneiro Vieira MLC (2008) Cytogenetic studies in some species of *Passiflora* L. (Passifloraceae): a review emphasizing brazilian species. Braz Arch Biol Technol 51:247–258. https://doi.org/10.1590/S1516-89132008000200003

Underwood CJ, Henderson IR, Martienssen RA (2017) Genetic and epigenetic variation of transposable elements in *Arabidopsis*. Curr Opin Plant Biol 36: 135-141. https://doi.org/ 10.1016/j.pbi.2017.03.002

Unfried I, Stocker U, Gruendler P (1989) Nucleotide sequence of the 18S rRNA gene from *Arabidopsis thaliana* Co10. Nucleic Acids Res 17:7513

Vicient CM, Casacuberta JM (2017) Impact of transposable elements on polyploid plant genomes. Ann Bot 120:195-207. https://doi.org/10.1093/aob/mcx078

Vitte C, Panaud O, Quesneville H (2007) LTR retrotransposons in rice (*Oryza sativa* L.): recent burst amplifications followed by rapid DNA loss. BMC Genomics 8:218. https://doi.org/ 10.1186/1471-2164-8-218

Xu Y, Du J (2014) Young but not relatively old retrotransposons are preferentially located in gene-rich euchromatic regions in tomato (*Solanum lycopersicum*) plants. Plant J 80:582-591. https://doi.org/10.1111/tpj.12656

Yotoko KS, Dornelas MC, Togni PD, Fonseca TC, Salzano FM, Bonatto SL, Freitas LB (2011) Does variation in genome sizes reflect adaptive or neutral processes? New clues from *Passiflora*. PLoS ONE 6:e18212. https://doi.org/10.1371/journal.pone.0018212

Zamudio N, Barau J, Teissandier A, Walter M, Borsos M, Servant N, Bourc'his D (2015) DNA methylation restrains transposons from adopting a chromatin signature permissive for meiotic recombination. Genes Dev 29:1256-1270. https://doi.org/ 10.1101/gad.257840.114

Zou J, Gong H, Yang TJ, Meng J (2009) Retrotransposons - a major driving force in plant genome evolution and a useful tool for genome analysis. J Crop Sci Biotechnol 12:1-8. https://doi.org/10.1007/s12892-009-0070-3